Effect of CaO-Al$_2$O$_3$-MgO Slags on the Formation of MgO-Al$_2$O$_3$ Inclusions in Ferritic Stainless Steel

JOO HYUN PARK and DONG SIK KIM

A thermodynamic equilibrium between the Fe-16Cr melts and the CaO-Al$_2$O$_3$-MgO slags at 1823 K as well as the morphology of inclusions was investigated to understand the formation behavior of the MgO-Al$_2$O$_3$ spinel-type inclusions in ferritic stainless steel. The calculated and observed activities of magnesium in Fe-16Cr melts are qualitatively in good agreement with each other, while those of aluminum in steel melts exhibit some discrepancies with scatters. In the composition of molten steel investigated in this study, the log ($X_{MgO}/X_{Al_2O_3}$) of the inclusions linearly increases by increasing the $\log\lfloor a_{Mg}/a_{Al}^2 \cdot a_O^2\rfloor$ with the slope close to unity. In addition, the relationship between the log ($X_{MgO}/X_{Al_2O_3}$) of the inclusions and the log ($a_{MgO}/a_{Al_2O_3}$) of the slags exhibits the linear correlation with the slope close to unity. The compositions of the inclusions are relatively close to those of the slags, *viz.* the MgO-rich magnesia-spinel solid solutions were formed in the steel melts equilibrated with the highly basic slags saturated by CaO or MgO. The spinel inclusions nearly saturated by MgO were observed in the steel melts equilibrated with the slags doubly saturated by MgO and MgAl$_2$O$_4$. The spinel and the Al$_2$O$_3$-rich alumina-spinel solid solutions were formed in the steel melts equilibrated with the slags saturated by MgAl$_2$O$_4$ and MgAl$_2$O$_4$-CaAl$_2$O$_4$ phases, respectively. The apparent modification reaction of MgO to the magnesium aluminate inclusions in steel melts equilibrated with the highly basic slags would be constituted by the following reaction steps: (1) diffusion of aluminum from bulk to the metal/MgO interface, (2) oxidation of the aluminum to the Al^{3+} ions at the metal/intermediate layer interface, (3) diffusion of Al^{3+} ions and electrons through the intermediate layer, and (4) magnesium aluminate (MgAl$_2$O$_4$ spinel, for example) formation by the ionic reaction.

I. INTRODUCTION

CHROMIUM stainless steels have widely been used for corrosion resisting materials at room or high temperatures as well as construction materials. However, the oxide inclusions such as spinel (MgAl$_2$O$_4$) probably deteriorate corrosion resistance and cause the surface defects and cracks during deep drawing or spinning manufacturing. Hence, some researchers have investigated the formation behavior of spinel in stainless steel melts for about the last 10 years.

Harkness and Dyson reported that the spinel, which has a stable fcc structure with high melting point, would readily form in stainless steel melts and this inclusion was not effectively suppressed by calcium addition from their plant data.[1] Kim *et al.* reported that the spinel phase could be crystallized in the suspended CaO-SiO$_2$-MgO-Al$_2$O$_3$(-TiO$_2$) inclusion matrix as the temperature of molten steel decreased from about 1923 K at AOD converter to about 1723 K at continuous casting mold.[2] From the analysis of plant data, they proposed that the aluminum content in steel melt and MgO content in AOD slag should be lowered to suppress the formation of spinel. The crystallization of spinel in the liquid CaO-SiO$_2$-MgO-Al$_2$O$_3$ inclusion matrix, with Al$_2$O$_3$ content greater than about 20 mass pct, has also recently been reported by Ehara *et al.*[3] However, in these works, the effect of slag compositions on the formation mechanism of spinel in molten steel has not been clearly understood.

Nishi and Shinme observed that the content of MgO in the Al$_2$O$_3$-based inclusions, readily formed by aluminum deoxidation, increased with increasing basicity ($\equiv$(pct CaO)/(pct SiO$_2$)) of the CaO-SiO$_2$-MgO-Al$_2$O$_3$ slags.[4] They proposed that the reduction of MgO in the slags by aluminum in molten steel at the slag/metal interface would provide small amounts of magnesium, which could react with Al$_2$O$_3$ inclusions, *albeit* less than 1 mass ppm magnesium. The similar mechanisms were suggested by Okuyama *et al.*[5] and Todoroki and Mizuno.[6] However, because the content of aluminum in molten steel was from about 0.01 to 1 mass pct in these studies, the initial inclusions were Al$_2$O$_3$, regardless of slag compositions. Furthermore, although the CaO-SiO$_2$-MgO-Al$_2$O$_3$ (-CaF$_2$) slags were reacted with the steel melts containing aluminum, only the reduction of MgO was considered. However, the SiO$_2$ could also be reduced by such a large content of aluminum, which was not taken into account.

Therefore, in the present study, the equilibrium reaction between the Fe-16Cr melts and the CaO-Al$_2$O$_3$-MgO slags was investigated to understand the formation behavior of the MgO-Al$_2$O$_3$ spinel-type inclusions in ferritic stainless steel under condition of aluminum content less than about 0.02 mass pct. The composition of the slags was chosen as the systems saturated by the solid phase for definite thermodynamic conditions.

II. EXPERIMENTAL

The pure iron and chromium were premelted in a vacuum induction furnace to make a composition of 16 mass pct Cr. The Fe-16Cr alloy of about 65 grams, the CaO-Al$_2$O$_3$-MgO slags of about 6 grams, and the small amounts of extra pure

JOO HYUN PARK, Senior Researcher, and DONG SIK KIM, Senior Researcher, are with the Stainless Steel Research Group, Technical Research Laboratories, POSCO, Pohang 790-785, Korea. Contact e-mail: basicity@posco.co.kr

manganese and silicon were charged into the pure MgO crucible, which were, then, located in a super kanthal electric furnace. In a commercial 16 mass pct Cr stainless steel, the contents of silicon and manganese are generally about 0.3 and 0.4 mass pct, respectively. The initial content of aluminum in the premelted Fe-16Cr alloy was less than about 20 ppm. In each run, the solid phase such as pure lime (>99.9 pct), MgO, MgAl$_2$O$_4$, CaAl$_2$O$_4$ was equilibrated with molten slags. These two solid phases were prepared from compacting and sintering at high temperatures and were confirmed by X-ray diffraction analysis.

A schematic diagram of the experimental apparatus is shown in Figure 1 and the experimental temperature was controlled to be 1823 ($\pm$2) K using an R-type (Pt-13Rh/Pt) thermocouple and a proportional integral differential controller. The oxygen as an impurity in an Ar gas was removed by passing the gas through titanium sponge heated to about 1173 K. The sponge titanium was also contained in the alumina holder, as shown in Figure 1, in order to minimize the oxygen contamination from the atmosphere. Thus, the oxygen partial pressure during the experiments was maintained to about $p_{O_2} = 10^{-19}$ to 10^{-18} atm, which was measured by the oxygen analyzer (Daiichi Nekken, model C-38, Hyogo, Japan).

The equilibration time was predetermined as about 2 hours. After equilibrating, the crucibles were quenched by Ar gas,
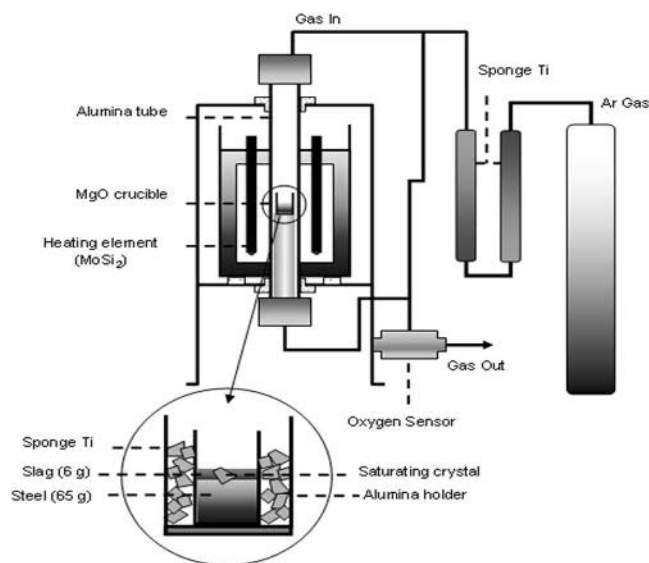
and were prepared for chemical analysis. The content of soluble aluminum, magnesium, and calcium was analyzed by the inductively coupled plasma (ICP) spectrometer (Spectro model FSPOAB3B, Kleve, Germany). An error of ICP analysis was less than about $\pm$5 pct. The total oxygen content in the sample was determined by fusion and the infrared absorption method. The composition of the slags was analyzed by an X-ray fluorescence spectrometer. The samples were mounted in cold-setting resin. Standard grinding and polishing techniques then were used, after which all samples were gold coated. Finally, the composition and morphology of about ten inclusions per sample were examined by backscattered electron imaging (BEI) and secondary electron imaging (SEI) using a SEM-EDS (model JSM-840A, JEOL,*)

---

*JEOL is a trademark of Japan Electron Optics Ltd., Tokyo.

---

with a link detector. The composition of inclusions in a specific run was taken from the average value of about ten inclusions.

The equilibrium compositions of the metals and slags after experiments are listed in Table I.
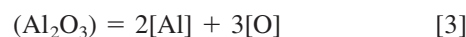
III. RESULTS AND DISCUSSION

A. Thermodynamics of Mg and Al in Fe-16Cr Melts Equilibrated with CaO-Al$_2$O$_3$-MgO Slags

The phase diagram and the liquid area of the CaO-Al$_2$O$_3$-MgO slag system at 1823 K are shown in Figure 2 with the experimental compositions.[7] As mentioned in Table I, each composition of the slag is saturated by CaO-MgO (①), MgO (θ) (② and ③), MgO-MgAl$_2$O$_4$ (④), MgAl$_2$O$_4$ (⑤), and MgAl$_2$O$_4$-CaAl$_2$O$_4$ (⑥), respectively.

The magnesium and aluminum in molten steel are, respectively, in equilibrium with the slags by the following equations.[8, 9]

$$(MgO) = [Mg] + [O] \quad [1]$$

$$\log K_{Mg} = \log a_{Mg} + \log a_O - \log a_{MgO} = -\frac{4700}{T} - 4.28 \quad [2]$$

$$(Al_2O_3) = 2[Al] + 3[O] \quad [3]$$

$$\log K_{Al} = 2\log a_{Al} + 3\log a_O - \log a_{Al_2O_3} = -\frac{45,300}{T} + 11.62 \quad [4]$$

Fig. 1—Experimental apparatus for the measurement of slag/metal equilibria.

Table I. Experimental Conditions and the Composition of the Fe-16Cr Steel Melts Investigated in the Present Study

| Number | Metal | | | | Slag | | | Conditions |
	[Pct Al]^{dissolved}	[Pct Mg]^{dissolved}	[Pct O]^{total}	[Pct O]^{dissolved,*}	(Pct MgO)	(Pct Al$_2$O$_3$)	(Pct CaO)	
SP-01	0.0070	0.0017	0.0022	0.00041	8.5	39.2	52.3	$a_{CaO} = a_{MgO} = 1$
SP-02	0.0075	0.0024	0.0013	0.00067	10.3	44.8	44.9	$a_{MgO} = 1$
SP-03	0.0124	0.0019	0.0006	0.00050	12.1	48.4	39.5	$a_{MgO} = 1$
SP-04	0.0062	0.0021	0.0012	0.00114	14.7	52.1	33.2	$a_{MgO} = a_{MgAl_2O_4} = 1$
SP-05	0.0062	0.0023	0.0015	0.00134	10.5	57.1	32.4	$a_{MgAl_2O_4} = 1$
SP-06	0.0201	0.0001	0.0017	0.00135	5.3	64.5	30.2	$a_{MgAl_2O_4} = a_{CaAl_2O_4} = 1$

[Si] = 0.3 mass pct, [Mn] = 0.4 mass pct, [Ca] < 0.0002 mass pct.
*Calculated value from [Al]-[O] equilibrium using alumina activity reported by Ohta and Suito.

where K_i is the equilibrium constant of Eqs. [1] and [3] for element i and a_i is the activity of i, of which standard state is the infinite dilute solution. The activity of magnesium, for example, in Fe-16Cr melts could be calculated by Eq. [5].

$$\log a_{Mg} = \log K_{Mg} - \log a_O + \log a_{MgO}$$

$$= \log K_{Mg} - (\log f_O + \log [\text{pct O}]) + \log a_{MgO}$$

$$= \log K_{Mg} - \sum_{M = Cr,Si,Mn,Mg,Al,O} (e_O^M \cdot [\text{pct M}]$$

$$+ r_O^M \cdot [\text{pct M}]^2) - \log [\text{pct O}] + \log a_{MgO} \qquad [5]$$

where f_O, e, and r are, respectively, the activity coefficient of oxygen in molten steel, and the first- and second-order interaction parameters, which are listed in Table II.[9–16] Hence, the effect of slag composition on the activity of magnesium in molten steel can be estimated from the activity of MgO in the slags equilibrated with Fe-16Cr steel melts. Similarly, the activity of aluminum can also be calculated. In the present study, the content of dissolved oxygen ([mass pct O]^{dissolved}) in Eq. [5] could be calculated from the aluminum-oxygen equilibria (Eqs. [3] and [4]) using the first- and second-order interaction parameters, the content of dissolved aluminum ([mass pct Al]^{dissolved}), and the activity of Al$_2$O$_3$ in the slags (Table I).[21]

Figure 3 exhibits the activities of magnesium calculated from Eq. [5] as a function of observed values, which were obtained from the measured contents (Table I) and the activity coefficients of magnesium in molten steel. Here, the activity of MgO in the CaO-Al$_2$O$_3$-MgO slags at 1823 K was
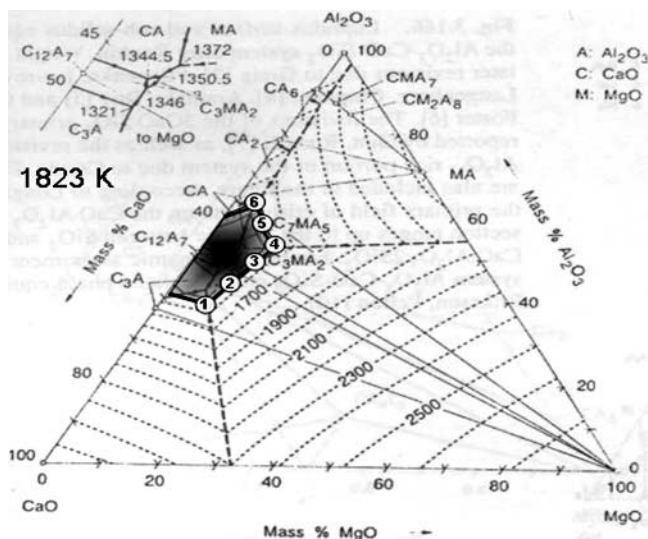
estimated from the data reported by Ohta and Suito[17] and Hino *et al*.[18] The regular solution behavior was assumed for extrapolating the activity data at 1873 K reported by Hino *et al*. to those at 1823 K. The calculated and observed activities of magnesium in Fe-16Cr melts are qualitatively in good agreement with each other. However, the calculated values using the activity of MgO reported by Hino *et al*. are slightly lower than the observed values. This discrepancy could be originated not only from the uncertainty in a_{MgO} in the CaO-Al$_2$O$_3$-MgO slags, especially in the low a_{MgO} region, but also from the interaction parameters between magnesium and oxygen in molten steel.

The calculated activities of aluminum in Fe-16Cr melts at 1823 K are shown in Figure 4 as a function of the observed values, which were obtained from the measured contents (Table I) and the activity coefficients of aluminum. Also, the activity of Al$_2$O$_3$ in the CaO-Al$_2$O$_3$-MgO slags at 1823 K was estimated from the data reported by Ohta and Suito[17] and Hino *et al*.[18] The regular solution behavior was also assumed for extrapolating the activity data reported by Hino *et al*. The calculated and observed activities of aluminum in Fe-16Cr melts exhibit some discrepancies with scatter. The values of the a_{Al} calculated from the $a_{Al_2O_3}$ reported by Ohta and Suito are slightly greater than the observed values and *vice versa* in the case of the a_{Al} calculated from the activity data by Hino *et al*. These discrepancies could be originated from the uncertainties in $a_{Al_2O_3}$ in the CaO-Al$_2$O$_3$-MgO slags.

B. Observations of MgO-Al$_2$O$_3$ Inclusions in Fe-16Cr Melts Equilibrated with CaO-Al$_2$O$_3$-MgO Slags

The formation of the magnesium aluminate inclusions can be discussed based on the thermodynamic equilibrium with magnesium, aluminum, and oxygen in the steel melts as follows:

$$(\text{MgO})^{inclusion} = [\text{Mg}] + [\text{O}] \qquad [6]$$

$$a_{MgO} = \frac{a_{Mg} \cdot a_O}{K_{Mg}} \qquad [7]$$

$$(\text{Al}_2\text{O}_3)^{inclusion} = 2[\text{Al}] + 3[\text{O}] \qquad [8]$$

$$a_{Al_2O_3} = \frac{a_{Al}^2 \cdot a_O^3}{K_{Al}} \qquad [9]$$

where a_i is the activity of i, and K_{Mg} and K_{Al} are, respectively, the equilibrium constant of Eqs. [6] and [8]. By combining Eqs. [7] and [9], the composition of inclusions can be deduced as a function of the activities of magnesium, aluminum, and oxygen as follows:

Fig. 2—Phase diagram of the CaO-Al$_2$O$_3$-MgO slag with the experimental compositions.[7]

$$\log\left(\frac{X_{MgO}}{X_{Al_2O_3}}\right) = \log\left[\frac{a_{Mg}}{a_{Al}^2 \cdot a_O^2}\right] - \log\left(\frac{\gamma_{MgO}}{\gamma_{Al_2O_3}}\right) + \log\left[\frac{K_{Al}}{K_{Mg}}\right] [10]$$

Table II. Interaction Parameters among Aluminum, Magnesium, and Oxygen

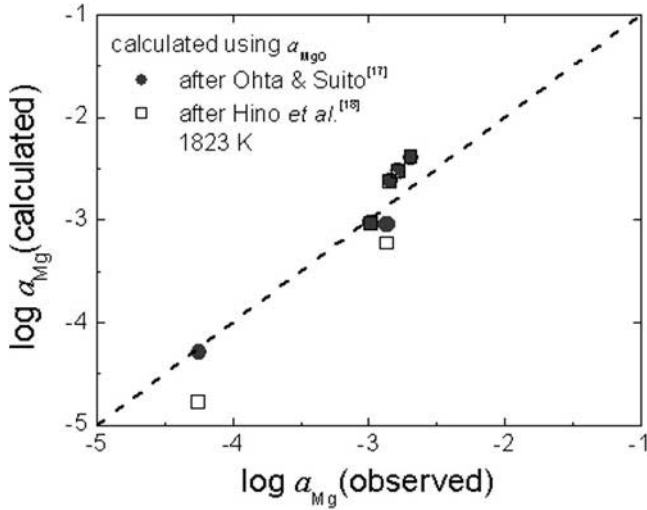| e_i^j (r_i^j)	Cr	Si	Mn	Al	Mg	O
Al	0.0096[11]	0.0056	0.035[12]	0.044	−0.3[13]	−2.122[9] (43.85)
Mg	0.0220[13]	−0.0960[13]	—	−0.270[13]		−560[14] (145,000)
O	−0.0330[15]	−0.0660	−0.037[16]	−1.254[9] (−0.0104)	−370[14] (5900)	−0.200

Fig. 3—Calculated activities of Mg in the Fe-16Cr melts equilibrated with the CaO-Al$_2$O$_3$-MgO slags at 1823 K as a function of observed values.
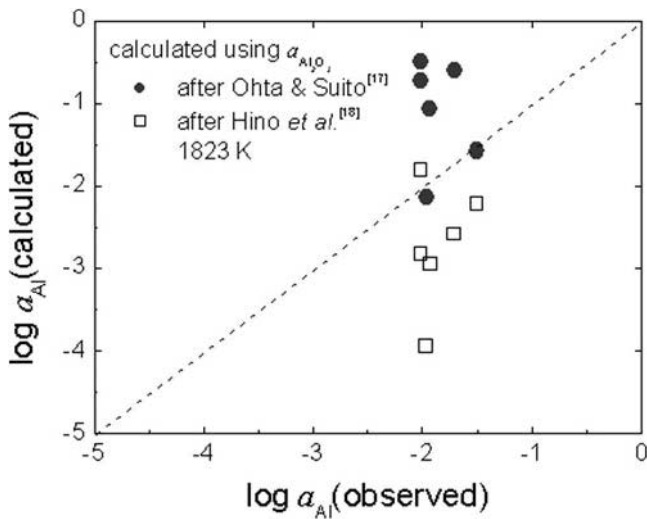

Fig. 5—Composition of inclusions, log ($X_{MgO}/X_{Al_2O_3}$) in Fe-16Cr melts as a function of log $\lfloor a_{Mg}/a_{Al}^2 \cdot a_O^2 \rfloor$ at 1823 K.

Fig. 4—Calculated activities of Al in the Fe-16Cr melts equilibrated with the CaO-Al$_2$O$_3$-MgO slags at 1823 K as a function of observed values.
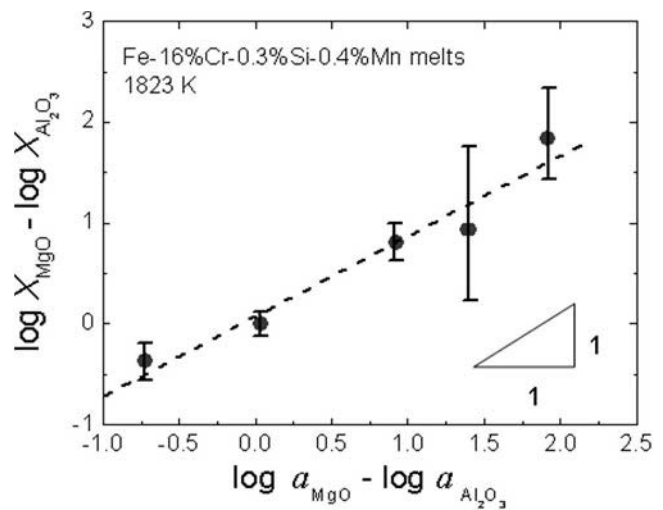
Fig. 6—Composition of inclusions, log ($X_{MgO}/X_{Al_2O_3}$) in Fe-16Cr melts as a function of log ($a_{MgO}/a_{Al_2O_3}$) at 1823 K.

where X_i and γ_i are the mole fraction and the activity coefficient of i in the inclusions. Hence, the ratio of MgO to Al$_2$O$_3$ of inclusions, log ($X_{MgO}/X_{Al_2O_3}$), is expected to exhibit a linear relation to the log $\lfloor a_{Mg}/a_{Al}^2 \cdot a_O^2 \rfloor$ with the slope of unity at a fixed temperature, if the activity coefficient term would not significantly be affected by steel compositions.

The ratio of X_{MgO} to $X_{Al_2O_3}$ of the inclusions in the Fe-16Cr melts equilibrated with the CaO-Al$_2$O$_3$-MgO slags at 1823 K is shown in Figure 5 as a function of the ratio of a_{Mg} to $a_{Al}^2 \cdot a_O^2$ in logarithmic scale. Here, the activities of magnesium, aluminum, and oxygen were calculated based on the slag/metal equilibria, as described in Section A using the thermodynamic data for the slag phase reported by Ohta and Suito.[17] In the composition of steel melts investigated in this study, the log ($X_{MgO}/X_{Al_2O_3}$) of the inclusions linearly increases by increasing the log $\lfloor a_{Mg}/a_{Al}^2 \cdot a_O^2 \rfloor$ with the slope of about 0.80, which is relatively close to unity. Furthermore, the relationship between the log ($X_{MgO}/X_{Al_2O_3}$) of the inclusions and

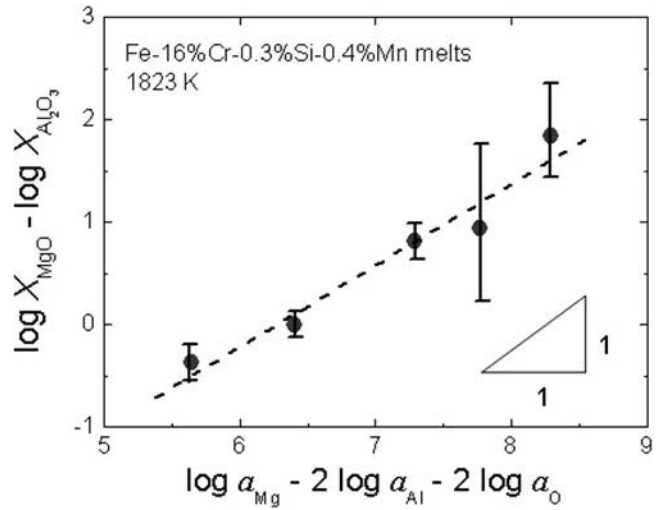the log ($a_{MgO}/a_{Al_2O_3}$) of the slags at 1823 K is shown in Figure 6, where the linear correlation between them with the slope close to unity is also observed. These phenomena could reveal that the slag/metal/inclusion system investigated in the present work is in the thermodynamic equilibrium and that the composition of the MgO-Al$_2$O$_3$ inclusions in the Fe-16Cr melts equilibrated with the CaO-Al$_2$O$_3$-MgO slags can be determined not only by the activities of the slag components but also by the activities of magnesium and aluminum in steel melts. This can easily be understood by comparing the compositions of the inclusions and slags as follows.

The average composition and the morphology of the representative MgO-Al$_2$O$_3$ inclusions in the Fe-16Cr melts equilibrated with the CaO-Al$_2$O$_3$-MgO slags are shown in Figure 7. The composition of the inclusions observed in the present study varies from about (mass pct MgO)/(mass pct Al$_2$O$_3$) = 1.2 (①) to 0.2 (⑥) in the MgO-Al$_2$O$_3$ phase diagram by changing the composition of the slags from the system doubly
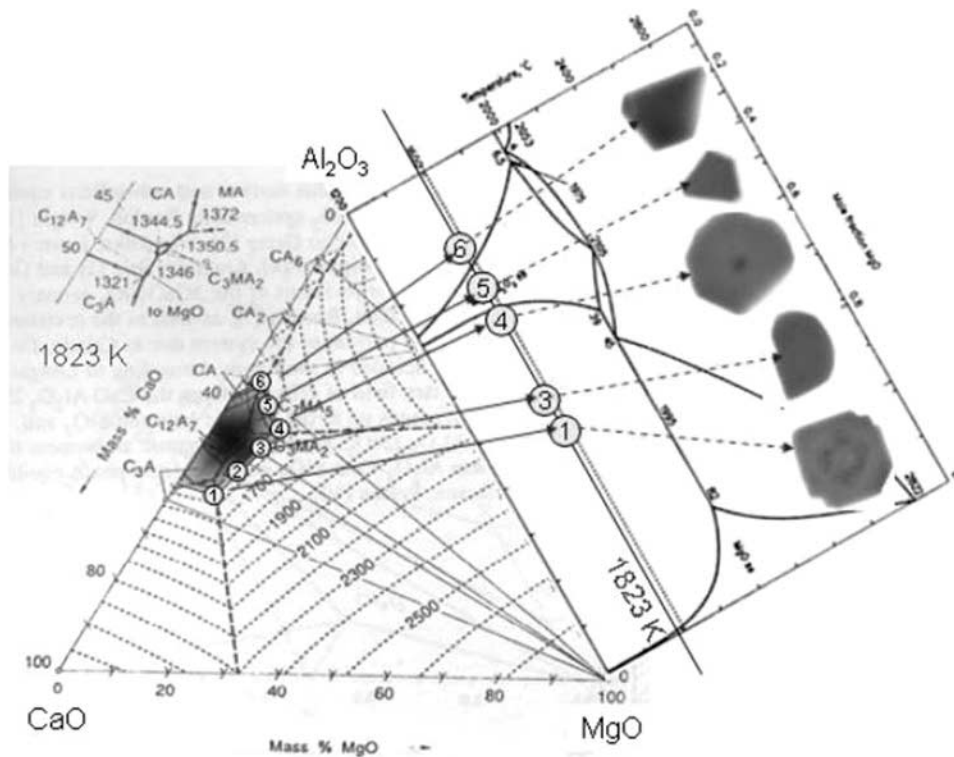
Fig. 7—Relationship between the compositions of inclusions and slags.

saturated by CaO and MgO to the system saturated by $MgAl_2O_4$-$CaAl_2O_4$ in the CaO-Al_2O_3-MgO ternary diagram. It is of interest that the compositions of the inclusions are relatively close to those of the slags, *viz.* the MgO-rich magnesia-spinel solid solutions were formed in the steel melts equilibrated with the highly basic slags saturated by CaO or MgO. The spinel inclusions nearly saturated by MgO were observed in the steel melts equilibrated with the slags doubly saturated by MgO and $MgAl_2O_4$ (④). Finally, the spinel (⑤) and the Al_2O_3-rich alumina-spinel solid solutions (⑥) were formed in the steel melts equilibrated with the slags saturated by $MgAl_2O_4$ and $MgAl_2O_4$-$CaAl_2O_4$ phases, respectively.

The relationship between the size and the composition of the MgO-Al_2O_3 inclusions in Fe-16Cr melts at 1823 K is shown in Figure 8. The size of the inclusions significantly decreases with increasing ratio of MgO to Al_2O_3, followed by constant values of about 1.5 to 2 μm. This is probably due to the difference in the interfacial properties between the Fe-Cr/Al_2O_3 and the Fe-Cr/MgO systems. Although there are interfacial properties between the Fe-16Cr melt and Al_2O_3,[19] there are no thermophysical data for the Fe-16Cr/MgO system. Thus, in this study, the contact angle and the work of adhesion of the ferrochrome melts are taken into account for comparison as follows.

The contact angle (θ) between ferrochrome melt and pure Al_2O_3 is about 90 deg and the work of adhesion (W_A) is about 1000 mJ/m^2, while the θ between ferrochrome and pure MgO is about 125 deg and the W_A is about 425 mJ/m^2 at 1923 K under an Ar atmosphere.[20] These physical properties indicate that the wettability of Al_2O_3 by the Fe-Cr melt is relatively greater than that of MgO. Hence, the clustering tendency of the Al_2O_3-rich inclusions would be larger than that of the MgO-rich inclusions in the molten Fe-Cr steel.
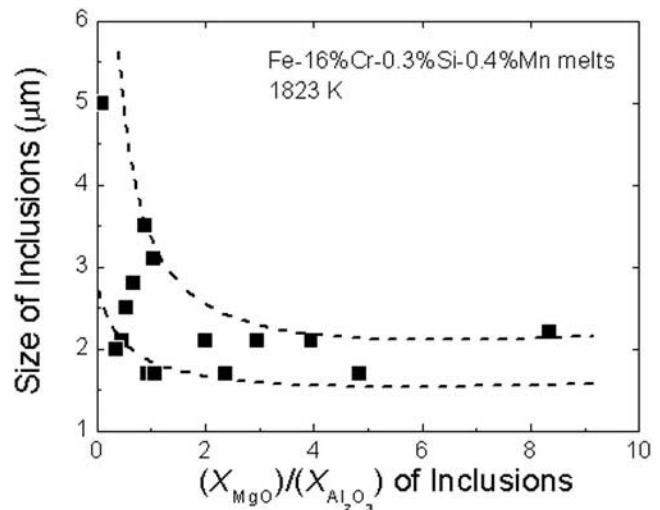

Fig. 8—Size of MgO-Al_2O_3 inclusions in Fe-16Cr melts at 1823 K as a function of inclusion composition.

C. Formation Mechanism of MgO-Al_2O_3 Inclusions in Fe-16Cr Melts Equilibrated with CaO-Al_2O_3-MgO Slags Doubly Saturated by CaO and MgO

The representative morphology of the inclusions in the Fe-16Cr melts equilibrated with the highly basic slags, *i.e.*, the CaO_{satd}-Al_2O_3-MgO_{satd} system at 1823 K, is shown in Figure 9. An EDS analysis and the element mapping results are also shown. The content of inclusions has been measured at three points from the center to the edge of the inclusions. It is of interest that the content of MgO and Al_2O_3 within the inclusions is not uniform but gradient, that is, the
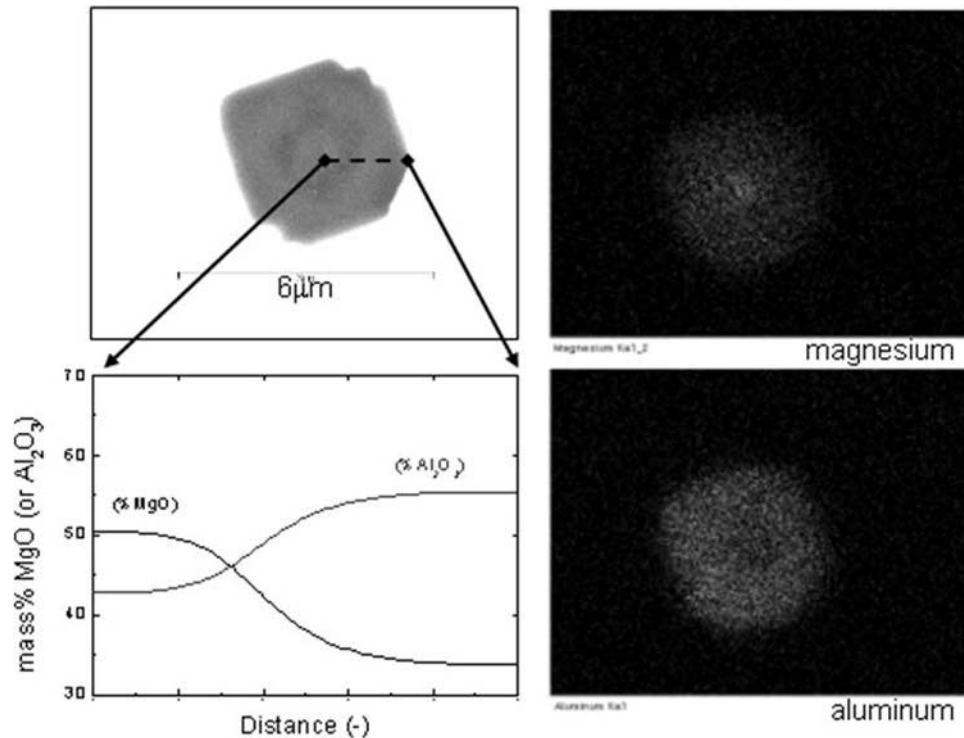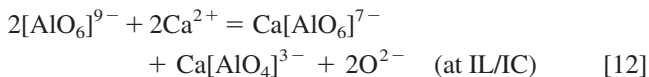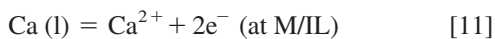
Fig. 9—Morphology and element mapping of the MgO-Al$_2$O$_3$ spinel-type inclusions in the Fe-16Cr melts equilibrated with the CaO$_{satd}$-Al$_2$O$_3$-MgO$_{satd}$ slags at 1823 K.

content of MgO decreases from about 50 mass pct at the center to about 35 mass pct at the edge of the inclusion, and *vice versa* in the case of Al$_2$O$_3$. This result probably indicates that the MgO particles would readily form in the Fe-16Cr melts equilibrated with the highly basic slags, followed by the reaction with aluminum at the MgO/metal interface, resulting in the transformation from MgO to MgO-Al$_2$O$_3$ complex inclusions. The element map of magnesium and aluminum could support the simple discussion mentioned previously. The formation mechanism of the MgO-Al$_2$O$_3$ inclusions in Fe-16Cr melts can be discussed in detail based not only on the measured results in this study but also on the modification mechanism of solid inclusions, newly developed in previous work.[21]

Recently, it has been proposed that the solid alumina particles in molten steel could be modified to liquid calcium aluminates by the following ionic exchange reactions at the metal/"intermediate layer" (M/IL) interface and at the intermediate layer/inclusion core (IL/IC) interface, respectively, as follows:[21]

$$Ca\ (l) = Ca^{2+} + 2e^- \quad (at\ M/IL) \qquad [11]$$

$$2[AlO_6]^{9-} + 2Ca^{2+} = Ca[AlO_6]^{7-}$$
$$+ Ca[AlO_4]^{3-} + 2O^{2-} \quad (at\ IL/IC) \qquad [12]$$

The modification mechanism of the MgO (periclase) inclusion, the structure of which is similar to that of corundum, that is, [MgO$_6$]-octahedra, to the MgO-Al$_2$O$_3$ system can similarly be described by employing the intermediate layer concept and can schematically be expressed in Figure 10. The apparent modification reaction of MgO inclusions would be constituted by the following reaction steps:
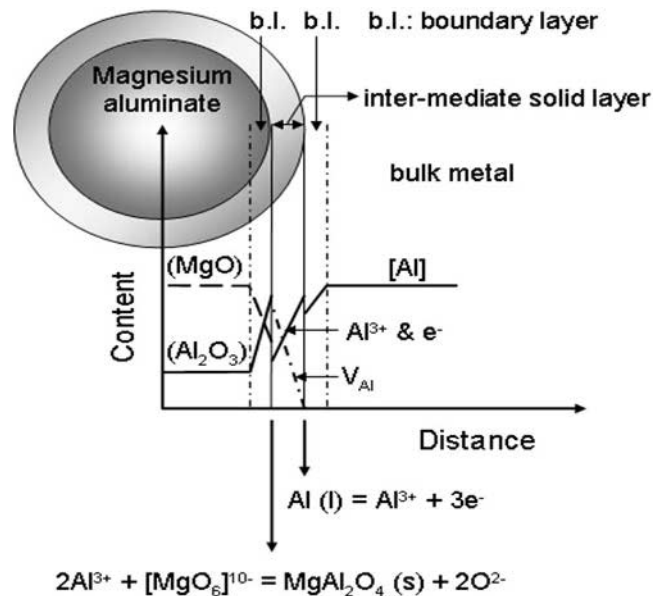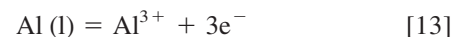

Fig. 10—Schematic diagram of the modification mechanism of MgO periclase by Al in molten Fe-16Cr steel.

(1) diffusion of aluminum atoms from bulk to the metal/MgO interface;
(2) oxidation of the aluminum atoms to the Al^{3+} ions at the metal/intermediate layer interface:

$$Al\ (l) = Al^{3+} + 3e^- \qquad [13]$$

(3) diffusions of Al^{3+} ions and charge-balancing electrons through the intermediate layer with the diffusion of equimolar vacancies (V_{Al}) to opposite direction; and

(4) magnesium aluminate ($MgAl_2O_4$ spinel, for example) formation by the reaction between Al^{3+} ions and $[MgO_6]^{10-}$-octahedral units at the IL/IC interface:

$$2Al^{3+} + [MgO_6]^{10-} = MgAl_2O_4(s) + 2O^{2-} \qquad [14]$$

The preceding mechanism of the inclusion modification is based not only on the crystal (and molecular) chemistry, which has been appeared in Pauling's integrated works, but also on the ionic/covalent characteristics of the interionic bonds in the solid (or liquid) oxide systems.[21,22,23] It has also been suggested that the crystallization of $MgAl_2O_4$ spinel phase in the glass-ceramics containing MgO and Al_2O_3 would be occur from the reaction between Mg^{2+}, which occupies the octahedral site, and Al^{3+} ions by employing the Fourier transform infrared, X-ray diffraction, and nuclear magnetic resonance analyses.[24,25]

In view of kinetics, the oxidation rate of aluminum atoms to Al^{3+} ions at the metal/intermediate layer interface (Eq. [13]) as well as the diffusion rate of Al^{3+} ions through this layer would be greater than that of $[MgO_6]$-octahedral units, *viz.* the diffusion rate of magnesium ions, in the boundary layer of the inclusion side. This qualitatively is in accordance with the formation kinetics of the MgO-spinel phase from the reaction between MgO and aluminum during the oxidation of the Al-Mg alloys at high temperatures suggested by Zayan *et al*.[26] They proposed that the diffusion of magnesium ions in the solid MgO-spinel solid solutions was a rate-controlling step by employing the surface analysis techniques such as X-ray photoelectron spectroscopy and Auger electron spectroscopy as well as scanning electron microscopy (SEM) and transmission electron microscopy. Therefore, the modification reaction, *viz.* the transformation from MgO periclase to MgO-Al_2O_3 spinel-type inclusions in molten steel equilibrated with the highly basic slags, could be assumed to occur at the IL/IC interface and could be controlled by the diffusion of magnesium, *i.e.*, $[MgO_6]$-octahedral units. However, it is proposed that the quantitative structural changes of magnesium aluminates at the interface between metal and inclusions should be investigated in the future in order to verify the modification mechanism of solid MgO inclusions discussed previously.

IV. CONCLUSIONS

A thermodynamic equilibrium between the Fe-16Cr melts and the CaO-Al_2O_3-MgO slags at 1823 K as well as the morphology of inclusions was investigated to understand the formation behavior of the MgO-Al_2O_3 spinel-type inclusions in ferritic stainless steel. The following conclusions were obtained.

1. The calculated and observed activities of magnesium in Fe-16Cr melts are qualitatively in good agreement with each other, while those of aluminum in steel melts exhibit some discrepancies with scatters.
2. In the composition of molten steel investigated in this study, the log $(X_{MgO}/X_{Al_2O_3})$ of the inclusions linearly increases by increasing the log $\lfloor a_{Mg}/a_{Al}^2 \cdot a_O^2 \rfloor$ with the slope close to unity. Furthermore, the relationship between the log $(X_{MgO}/X_{Al_2O_3})$ of the inclusions and the log $(a_{MgO}/a_{Al_2O_3})$ of the slags exhibits the linear correlation with the slope close to unity.

3. The compositions of the inclusions are relatively close to those of the slags, *viz.* the MgO-rich magnesia-spinel solid solutions were formed in the steel melts equilibrated with the highly basic slags saturated by CaO or MgO. The spinel inclusions nearly saturated by MgO were observed in the steel melts equilibrated with the slags doubly saturated by MgO and $MgAl_2O_4$. The spinel and the Al_2O_3-rich alumina-spinel solid solutions were formed in the steel melts equilibrated with the slags saturated by $MgAl_2O_4$ and $MgAl_2O_4$-$CaAl_2O_4$ phases, respectively.
4. The size of the inclusions significantly decreases with increasing ratio of MgO to Al_2O_3, followed by constant values of about 1.5 to 2 μm. This is probably due to the difference in the interfacial properties between the Fe-Cr/Al_2O_3 and the Fe-Cr/MgO systems.
5. The apparent modification reaction of MgO to the magnesium aluminate inclusions in steel melts equilibrated with the highly basic slags would be constituted by the following reaction steps:

   (a) diffusion of aluminum from the bulk to the metal/MgO interface;
   (b) oxidation of the aluminum to the Al^{3+} ions at the metal/intermediate layer interface;
   (c) diffusion of Al^{3+} ions and electrons through the intermediate layer; and
   (d) magnesium aluminate ($MgAl_2O_4$ spinel, for example) formation by the ionic reaction.

REFERENCES

1. B. Harkness and D. Dyson: *Proc. METEC Cong. '94*, Düsseldorf, June 20–22, 1994, VDEh, Düsseldorf, 1994, pp. 70-77.
2. J.W. Kim, S.K. Kim, D.S. Kim, Y.D. Lee, and P.K. Yang: *Iron Steel Inst. Jpn. Int.*, 1996, vol. 36, pp. S140-S143.
3. Y. Ehara, S. Nakamura, and Y. Habara: *Proc. 4th Eur. Stainless Steel Science and Market Cong.*, Paris, Jun. 10–13, 2002, ATS, Paris, 2002, vol. 2, pp. 176-81.
4. T. Nishi and K. Shinme: *Tetsu-to-Hagané*, 1998, vol. 84, pp. 837-43.
5. G. Okuyama, K. Yamaguchi, S. Takeuchi, and K. Sorimachi: *Iron Steel Inst. Jpn. Int.*, 2000, vol. 40, pp. 121-28.
6. H. Todoroki and K. Mizuno: *Trans. ISS*, 2003, Mar., pp. 60-67.
7. M. Kowalski, P.J. Spencer, and D. Neuschutz: *Slag Atlas*, 2nd ed., Verlag Stahleisen GmbH, Düsseldorf, 1995.
8. H. Itoh, M. Hino, and S. Ban-ya: *Tetsu-to-Hagané*, 1997, vol. 83, pp. 623-28.
9. H. Itoh, M. Hino, and S. Ban-ya: *Tetsu-to-Hagané*, 1997, vol. 83, pp. 773-78.
10. *Steelmaking Data Sourcebook*, The Japan Society for the Promotion of Science, The 19th Committee of Steelmaking, Gordon and Breach Science Publications, New York, NY, 1988, pp. 273-325.
11. H. Ohta and H. Suito: *Iron Steel Inst. Jpn. Int.*, 2003, vol. 43, pp. 1301-08.
12. Z. Hong, X. Wu, and C. Kun: *Steel Res.*, 1995, vol. 66, pp. 72-76.
13. S.K. Jo, B. Song, and S.H. Kim: *Metall. Mater. Trans. B*, 2002, vol. 33B, pp. 703-09.
14. J.D. Seo and S.H. Kim: *Steel Res.*, 2000, vol. 71, pp. 101-06.

15. T. Itoh, T. Nagasaka, and M. Hino: *Iron Steel Inst. Jpn. Int*., 2000, vol. 40, pp. 1051-58.
16. K. Takahashi and M. Hino: *High Temp. Mater. Proc*., 2000, vol. 19, pp. 1-10.
17. H. Ohta and H. Suito: *Iron Steel Inst. Jpn. Int*., 1996, vol. 36, pp. 983-90.
18. M. Hino, S. Kinoshita, Y. Ehara, H. Itoh, and S. Ban-ya: *Proc. 5th. Int. Conf. Molten Slags, Fluxes and Salts '97*, Sydney, Jan. 5–8, 1997, ISS-AIME, Warrendale, PA, 1997, pp. 53-57.
19. K. Mukai, Z. Li, and M. Zeze: *Mater. Trans*., 2002, vol. 43, pp. 1724-31.
20. B.J. Keene: *Slag Atlas*, 2nd ed., Verlag Stahleisen GmbH, Düsseldorf, 1995, pp. 513-40.
21. J.H. Park, D.S. Kim, and S.B. Lee: *Metall. Mater. Trans. B*, 2005, vol. 36B, pp. 67-73.
22. L. Pauling: *The Nature of the Chemical Bond and the Structure of Molecules and Crystals: An Introduction to Modern Structural Chemistry*, 3rd ed., Cornell University Press, New York, NY, 1960, pp. 64-107.
23. J.H. Park and D.J. Min: *Metall. Mater. Trans. B*, 2001, vol. 32B, pp. 297-303.
24. J. Livage, F. Babonneau, M. Chatry, and L. Coury: *Ceram. Int*., 1997, vol. 23, pp. 13-18.
25. M.K. Naskar and M. Chatterjee: *J. Eur. Ceram. Soc*., 2004, vol. 24, pp. 3499-3508.
26. M.H. Zayan, O.M. Jamjoom, and N.A. Razik: *Oxid. Met*., 1990, vol. 34, pp. 323-33.